Fluorescence Quenching Studies of the Interaction of a Pyrene-Labeled Polyelectrolyte with Quencher-Carrying Oppositely Charged Micelles

Masanobu Mizusaki and Yotaro Morishima*

Department of Macromolecular Science, Osaka University, Toyonaka, Osaka 560, Japan

Katsunori Yoshida† and Paul L. Dubin

Department of Chemistry, Indiana University-Purdue University at Indianapolis, Indianapolis, Indiana 46205-2820

Received July 14, 1997. In Final Form: October 7, 1997⊗

The interaction between poly(sodium 2-(acrylamido)-2-methylpropanesulfonate) labeled with 1 mol % pyrene (PyPAMPS) and mixed micelles of hexaethylene glycol *n*-dodecyl monoether ($C_{12}E_6$) and *n*-hexadecyltrimethylammonium chloride (CTAC), in which *N*,*N*-dimethylaniline (DMA) was solubilized, was studied by steady-state and time-dependent fluorescence quenching by varying the mole fraction of CTAC (Y) in the mixed micelle. At $Y < 0.05$, fluorescence quenching is essentially dynamic, arising from collisional encounters of the pyrene sites and DMA-carrying mixed micelles. Strong quenching begins to occur at $Y \cong 0.05$, corresponding to the onset of polyelectrolyte−micelle interactions. In the region $0.05 < Y < 0.09$, the quenching was shown to occur via transient complex formation between PyPAMPS and the mixed micelle. Changes in the vibrational structures of fluorescence spectra of pyrene in PyPAMPS indicate that pyrene groups are inserted in the hexa(oxyethylene) phase of the mixed micelle when the polymer−micelle complex is formed. The extent of quenching reaches a limiting value at $Y > 0.11$ in excess micelle solution, corresponding to the state in which all pyrene groups are micelle-bound.

Introduction

Systems containing polyelectrolytes and ionic surfactant micelles may serve as models for the interaction of polyelectrolytes with oppositely charged particles. Such interactions are important in biological phenomena, e.g., the nonspecific association of DNA with basic proteins,[1] the immobilization of enzymes in polyelectrolyte complexes,[2] and the purification of proteins by selective precipitation and coacervation.[3] Polyelectrolyte−colloid interactions are also important in commercial processes, which include water treatment by colloidal flocculation,[4] the treatment of mineral suspensions,[5] and the stabilization of concentrated preceramic suspensions.[6]

Early studies on polymer−surfactant systems mainly focused on mixtures of nonionic polymers and ionic micelles, or polyelectrolytes and surfactant monomers, leading to a great variety of experimental data.[7] However, reports concerning the interaction of polyelectrolytes with surfactant micelles of opposite charge were relatively few until recently. This is because polyelectrolytes interact with oppositely charged surfactant micelles so strongly that irreversible macroscopic phase separation usually occurs. Dubin and co-workers[8] showed that such strong electrostatic interactions could be reduced by "diluting" the surface charge of ionic surfactant micelles with nonionic surfactants, leading to the formation of soluble polyelectrolyte−micelle complexes. Complex formation occurs abruptly when the micellar surface charge density reaches a certain critical level.[8−12] This critical micelle charge density only depends on the ionic strength and polymer linear charge density and is independent of the concentrations of polyelectrolytes and micelles.[8−12] Such phase-transition-like behavior is consistent with theoretical predictions for the interaction of polyelectrolytes with oppositely charged surfaces[13−17] and with recent simulations.[18] The micelle charge density of ionic/nonionic mixed micelles can be experimentally manipulated via the mole fraction (Y) of ionic surfactant. Accordingly, results obtained with polyelectrolyte−mixed micellar systems may be compared with theories for polyion−colloid interactions.

Optically clear polyelectrolyte−mixed micelle solutions abruptly become strongly turbid at a critical micelle surface charge density (Y_p) due to macroscopic phase

† Permanent address: Shiseido Basic Research Laboratories, Yokohama, 223 Japan.

⊗ Abstract published in *Advance ACS Abstracts,* November 15, 1997.

(1) See, for example: Shaner, S. L.; Melancon, P.; Lee, K. S.; Burgess, R. R.; Record, M. T., Jr. *Cold Spring Harbor Symp. Quant. Biol.* **1983**, *47*, 463.

(2) Margolin, A.; Sheratyuk, S. F.; Izumrudov, V. A.; Zezin, A. B.; Kabanov, V. A. *Eur. J. Biochem.* **1985**, *146*, 625.

(3) Strege, M. A.; Dubin, P. L.; West, J. S.; Daniel Flinta, C. D. In *Protein Purification: from Molecular Mechanisms to Large-Scale Processes*; Ladisch, M., Willson, R. C., Painton, C. C., Builder, S. E., Eds.; American Chemical Society: Washington, DC, 1990; Chapter 5.

(4) Schwoyer, W. L. K., Ed. *Polyelectrolytes for Water and Wastewater Treatment*; CRC Press: Boca Raton, FL, 1981.

(5) Read, A. D. *Br. Polym. J.* **1972**, *4*, 253.

(6) Cesarano, J., III; Aksay, I. A. *J. Am. Chem. Soc.* **1988**, *71*, 1062.

(7) See, for example: (a) Li, Y.; Dubin, P. L. In *Structure and Flow in Surfactant Solutions*; Herb, C. A.; Prud'homme, R. K., Eds., ACS Symposium Series 578; American Chemical Society: Washington, DC 1994; Chapter 23, p 320. (b) Goddard, E. D. *J. Am. Oil . Chem. Soc.* **1994**, *71*, 1. (c) Wei, Y. C.; Hudson, S. M. *J. Macromol. Sci.-Rev. Macromol. Chem. Phys.* **1995**, *35*, 15. (d) Brackman, J. C.; Engberts, J. B. F. N. *Chem. Soc. Rev.* **1993**, *22*, 85.

(8) See, for example: Dubin, P. L.; Rigsbee, D. R.; Gan, L. M.; Fallon, M. A. *Macromolecules* **1988**, *21*, 2555.

(9) McQuigg, D. W.; Kaplan, J. I.; Dubin, P. L. *J. Phys. Chem.* **1992**, *96*, 1973.

(10) Li, Y.; Dubin, P. L.; Dautzenberg, H.; Lück, U.; Hartmann, J.; Tuzar, Z. *Macromolecules* **1995**, *28*, 6795.

(11) Li, Y.; Dubin, P. L.; Havel, H. A.; Edwards, S. L.; Dautzenberg, H. *Macromolecules* **1995**, *28*, 3098.

(12) Xia, J.; Zhang, H.; Rigsbee, D. R.; Dubin, P. L.; Shaikh, T. *Macromolecules* **1993**, *26*, 2759.

(13) Wiegel, F. W. *J. Phys. A: Math. Gen.* **1977**, *10*, 299.

(14) Evers, O. A.; Fleer, G. J.; Scheutjens, J. M. H. M.; Lyklema, J. *J. Colloid Interface Sci.* **1986**, *111*, 446.

(15) Muthukumar, M. *J. Chem. Phys.* **1987**, *86*, 7230.

(16) Odijk, T. *Langmuir* **1991**, *7*, 1991.

(17) von Goeler, F.; Muthukumar, M. *J. Chem. Phys.* **1994**, *100*, 7796.

(18) Muthukumar, M. *J. Chem. Phys.* **1995**, *103*, 4723.

S0743-7463(97)00780-4 CCC: $14.00

separation. Below Y_p, however, a critical micelle charge density (Y_c) is observed at which soluble polyelectrolyte-micelle complexes are formed.[8,10−12] The structure of such soluble polymer−micelle complexes may be studied by a variety of experimental techniques including turbidimetric titration[8] and light scattering.[10−12] Especially, static[12,19] and quasielastic[8,10,11,19] light scattering (QELS) have provided important information on the size and structure of polymer−micelle complexes. However, such soluble complexes can only be detected by QELS if their lifetime (residence time of bound micelles on a polymer) is sufficiently long and the scattering intensity of the complexes is sufficiently large compared with those of the micelles and polymers from which they form.

In contrast to QELS, fluorescence techniques can detect transient soluble complexes formed between polyelectrolytes and micelles even though their mass is comparable to those of the polyelectrolytes and micelles. One of our primary interests here is an experimental verification of dynamic processes in the formation of such soluble complexes and the utilization of fluorescence techniques to gain insight into such transient species. Therefore, we examined the interaction of a pyrene-labeled polyanion with cationic/nonionic mixed micelles in which a quencher is solubilized.

Experimental Section

Materials. The pyrene-labeled poly(sodium 2-(acrylamido)-2-methylpropanesulfonate) (PyPAMPS) was prepared by copolymerization of 2-(acrylamido)-2-methylpropanesulfonic acid (AMPS) and *N*-(1-pyrenylmethyl)methacrylamide as reported previously.[20] The content of the pyrene unit in the copolymer

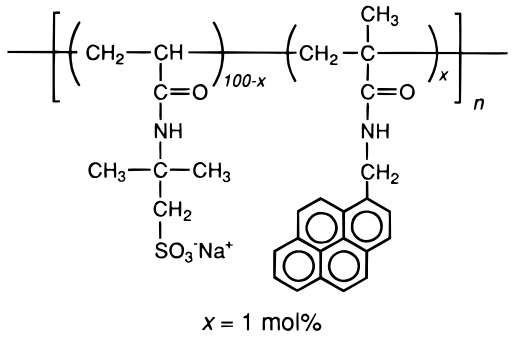

PyPAMPS

was determined to be 1 mol % by UV absorbance at 343 nm. This low mole percent of pyrene in the polymer assures the existence of isolated pyrene chromophores with minimal alteration of polyelectrolyte properties. Molecular weight of PyPAMPS was estimated to be 4×10^4 by size exclusion chromatography (SEC) on Superose 6 columns, relative to pullulan standards.

Hexaethylene glycol *n*-dodecyl monoether ($C_{12}E_6$) (Nikko Chemical) was used without further purification. A high purity of $C_{12}E_6$ was confirmed by high-performance liquid chromatography (HPLC). *n*-Hexadecyltrimethylammonium chloride (CTAC) (Wako Pure Chemicals) was recrystallized twice from methanol. *N*,*N*-Dimethylaniline (DMA) (Aldrich) was purified by distillation under reduced pressure. NaCl (Wako Pure Chemicals) was used without further purification. Milli-Q water was used for the turbidimetric titration and fluorescence measurements.

Turbidimetric Titration. Turbidimetric titrations were carried out at 420 nm with a JASCO V-520 spectrophotometer with a 1-cm path length quartz cuvette. "Type I" turbidimetric titrations,[8,12,21−24] which involve addition of a solution of 50 mM CTAC to a mixture of 0.05 g/L polymer and 30 mM $C_{12}E_6$, were performed at a constant ionic strength at 25 ± 1 °C. The ionic strengths were adjusted with NaCl. All transmittance values were corrected by subtracting the turbidity of a polymer-free blank. The blank-corrected turbidity (here approximated by 100 − %T) was plotted as a function of Y, the mole fraction of the cationic surfactant, defined as $Y = \{[CTAC]/([CTAC] + [C_{12}E_6])\}$.

Fluorescence Quenching. A DMA-saturated aqueous solution was prepared as follows. A mixture of 0.247 g (2.04 mmol) of DMA and 88.0 mL of pure water was sonicated for 2 h and magnetically stirred for an additional 3 h at room temperature. After allowing the mixture to stand overnight, a small portion of the aqueous layer was carefully sucked up with a syringe and slowly filtered with a 0.1 μm Millipore filter. The concentration of the DMA-saturated aqueous solution was determined to be 7.51 mM from the absorbance of a diluted solution at 243 nm, using the molar extinction coefficient in methanol ($\epsilon = 1.08 \times 10^4$ M^{-1}) which had been determined in a separate experiment.

For fluorescence quenching experiments in micelle-free solution, predetermined amounts of the DMA-saturated solution were mixed with stock solutions of 2.01 g/L PyPAMPS and 2 M NaCl, and the mixture was diluted with pure water so that the concentrations of PyPAMPS and NaCl were adjusted to 0.05 g/L and 0.2 M, respectively, the DMA concentrations varying from 0 to 5.00 mM. For the quenching experiments in the presence of $C_{12}E_6$, a mixture of predetermined amounts of the stock solutions of 7.51 mM DMA, 2.01 g/L PyPAMPS, 137 mM $C_{12}E_6$, and 2 M NaCl was diluted with pure water such that the concentrations of PyPAMPS, $C_{12}E_6$, and NaCl were adjusted to 0.05 g/L, 30 mM, and 0.2 M, respectively, the DMA concentrations varying from 0 to 4.91 mM. To prepare a DMA-carrying $C_{12}E_6$ micelle stock solution, a predetermined amount of DMA was added to a known amount of a 137 mM $C_{12}E_6$ solution, and the solution was stirred overnight. For type I fluorescence titration, a solution of 50 mM CTAC in 0.2 M NaCl was added to a water-diluted mixture of predetermined amounts of the PyPAMPS, DMA-solubilized $C_{12}E_6$, and NaCl stock solutions.

Steady-state fluorescence spectra were recorded on a Hitachi F-4500 fluorescence spectrophotometer with excitation at 343 nm. A complete run of quenching experiments to obtain a Stern−Volmer plot was performed within a period of 3 h to avoid a drift of the sensitivity of the instrument.

Fluorescence decays were measured by a time-correlated single-photon counting technique using a Horiba NAES 550 system equipped with a flash lamp filled with H_2. The decay function and response function were both measured simultaneously. The decay curves were analyzed by conventional deconvolution techniques. Sample solutions were the same as those used for the steady-state fluorescence measurements.

Results and Discussion

Fluorescence Quenching in Micelle-Free Aqueous Solution. Fluorescence of pyrene is known to be quenched by DMA in nonpolar media by exciplex formation or in polar media by electron transfer.[25] Figure 1 shows Stern−Volmer plots for the quenching of PyPAMPS by DMA in 0.2 M NaCl observed by steady-state and time-dependent fluorescence. Here, I_0 and I are the steady-state fluorescence intensities in the absence and presence of DMA and τ_0 and τ are the fluorescence lifetimes in the absence and presence of DMA, respectively. The plots for I_0/I and τ_0/τ appear to be linear, but the slope for the τ_0/τ plot is smaller than that for the I_0/I plot. These observations are indicative of a mix of dynamic and static quenching.[26] The static quenching may be due to a ground-state donor−acceptor interaction between pyrene and DMA.

(19) Dubin, P. L.; Thé, S. S.; Gan, L. M.; Chew, C. H. *Macromolecules* **1990**, *23*, 2500.
(20) Morishima, Y.; Tominaga, Y.; Kamachi, M.; Okada, T.; Hirata, Y.; Mataga, N. *J. Phys. Chem.* **1991**, *95*, 6027.
(21) Dubin, P. L.; Chew, C. H.; Gan, L. M. *J. Colloid Interface Sci.* **1989**, *128*, 566.
(22) Dubin, P. L.; Vea, M. E. Y.; Fallon, M. A.; Thé, S. S.; Rigsbee, D. R.; Gan, L. M. *Langmuir* **1990**, *6*, 1422.
(23) Dubin, P. L.; Davis, D. *Colloids Surf.* **1985**, *13*, 113.
(24) Dubin, P. L.; Thé, S. S.; McQuigg, D. W.; Chew, C. H.; Gan, L. M. *Langmuir* **1989**, *5*, 89.
(25) Lakowicz, J. R. In *Principles of Fluorescence Spectroscopy*; Plenum Press: New York and London, 1983; Chapter 9.
(26) Birks, J. B. In *Photophysics of Aromatic Molecules*; Wiley-Interscience: London and New York, 1970; Chapter 9.

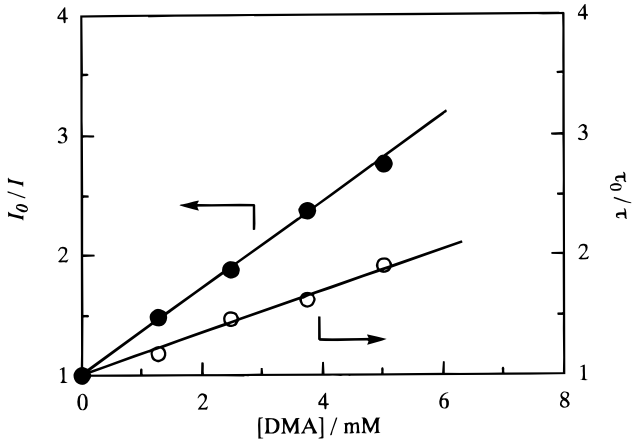

Figure 1. Stern−Volmer plots for fluorescence quenching of PyPAMPS by DMA in 0.2 M NaCl: [PyPAMPS] = 0.05 g/L.

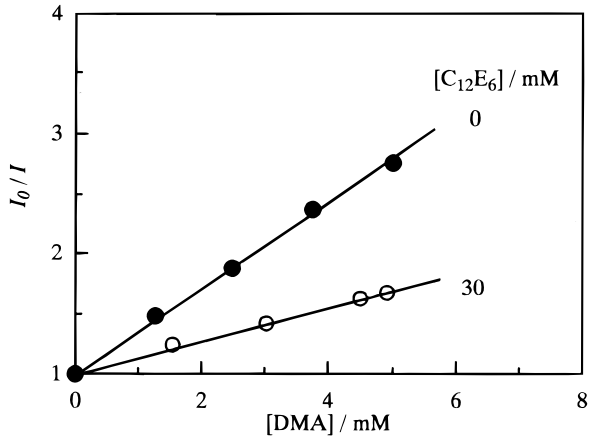

Figure 2. Stern−Volmer plots for fluorescence quenching of PyPAMPS by DMA in the absence (●) and presence (○) of 30 mM $C_{12}E_6$ in 0.2 M NaCl: [PyPAMPS] = 0.05 g/L.

Fluorescence Quenching in the Presence of $C_{12}E_6$ Micelle. The extent of fluorescence quenching is considerably decreased by the addition of $C_{12}E_6$. Figure 2 compares Stern−Volmer plots in the absence and presence of 30 mM $C_{12}E_6$ in 0.2 M NaCl. The addition of 30 mM $C_{12}E_6$ (micellar concentration is 1.0×10^{-4} M, assuming an aggregation number of 3.0×10^2 at 25 °C[27]) decreased the quenching more than 2-fold. Two extreme cases may be invoked to explain these observations: (1) all DMA molecules are completely solubilized in the micelles and fluorescence quenching is due to dynamic encounters of pyrene labels and DMA-solubilized $C_{12}E_6$ micelles, and (2) only some of the DMA molecules are solubilized in the micelles, the observed quenching being mainly due to free DMA species in the bulk aqueous phase.

Although the slope of the plot in the presence of $C_{12}E_6$ in Figure 2 appears to be constant, its physical meaning is rather complicated because the number of DMA molecules solubilized in micelles varies with the concentration of DMA. In order to differentiate between these two cases, we performed a quenching experiment under conditions where the micelle concentration was varied, keeping the DMA:surfactant stoichiometry fixed at a value corresponding to a constant number of DMA molecules per micelle (n). The value of n was calculated from the concentrations of the micelle and DMA, assuming that all DMA molecules are completely solubilized in the micelle. Results for $n = 9.4$ are plotted in Figure 3, which shows that the steady-state and time-dependent fluorescence

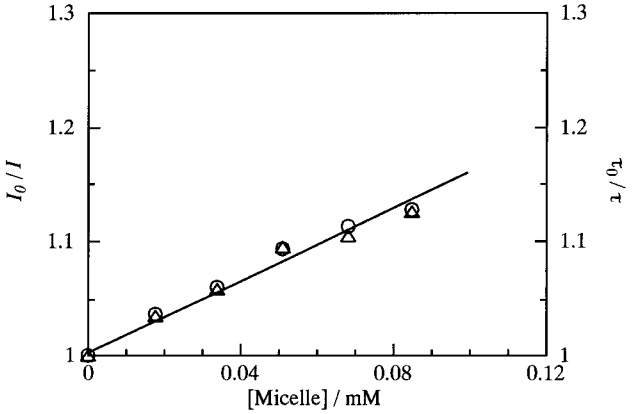

Figure 3. Stern−Volmer plots for steady-state (○) and time-dependent (△) fluorescence quenching of PyPAMPS by DMA at varying $C_{12}E_6$ concentrations in 0.2 M NaCl: [PyPAMPS] = 0.05 g/L and $n = 9.4$.

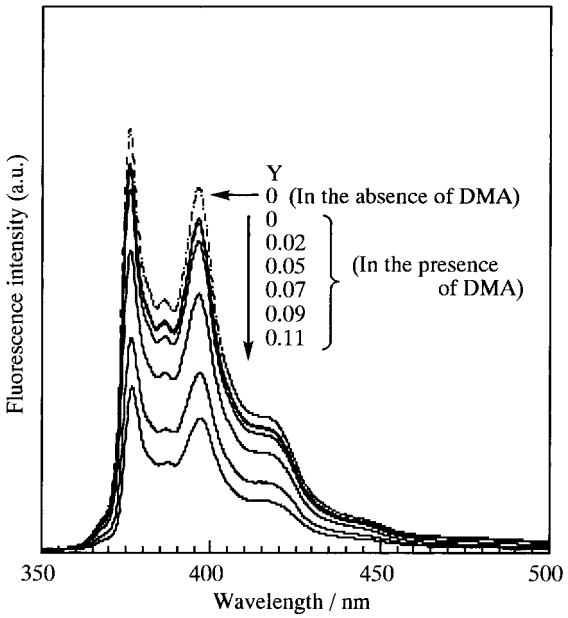

Figure 4. Fluorescence spectra at varying Y for PyPAMPS in the absence and presence of DMA-carrying $C_{12}E_6$/CTAC mixed micelle: [PyPAMPS] = 0.05 g/L, $[C_{12}E_6] = 30$ mM, $n = 9.4$, and [NaCl] = 0.2 M.

quenching plots coincide. This indicates that the quenching is essentially dynamic and is due to collisions between pyrene sites and DMA-carrying $C_{12}E_6$ micelles.[28]

Fluorescence Quenching in the Presence of $C_{12}E_6$/CTAC Mixed Micelles. Results in Figure 3 suggest that when a DMA-solubilized micelle encounters a pyrene site in PyPAMPS, the pyrene group enters the micellar phase, leading to quenching of pyrene fluorescence. Figure 4 compares fluorescence spectra for the pyrene label in the presence of DMA-carrying $C_{12}E_6$/CTAC mixed micelles at varying Y under conditions of $[C_{12}E_6] = 30$ mM and $n = 9.4$. A fluorescence spectrum in the presence of 30 mM of quencher-free micelles at $Y = 0$ is also presented for comparison. The fluorescence intensity decreases slightly as Y is increased from 0 to ca. 0.05 owing to collisions between pyrene sites and DMA-carrying $C_{12}E_6$/CTAC mixed micelles and then decreases substantially as Y is further increased.

Figure 5 shows the results of type I titrations, in which the incremental addition of CTAC is reported as Y,

(27) Lianos, P.; Zana, R. *J. Colloid Interface Sci.* **1981**, *84*, 100.

(28) Turro, N. J. In *Modern Molecular Photochemistry*; Benjamin/Cummings: Menlo Park, CA, 1978; Chapter 8.

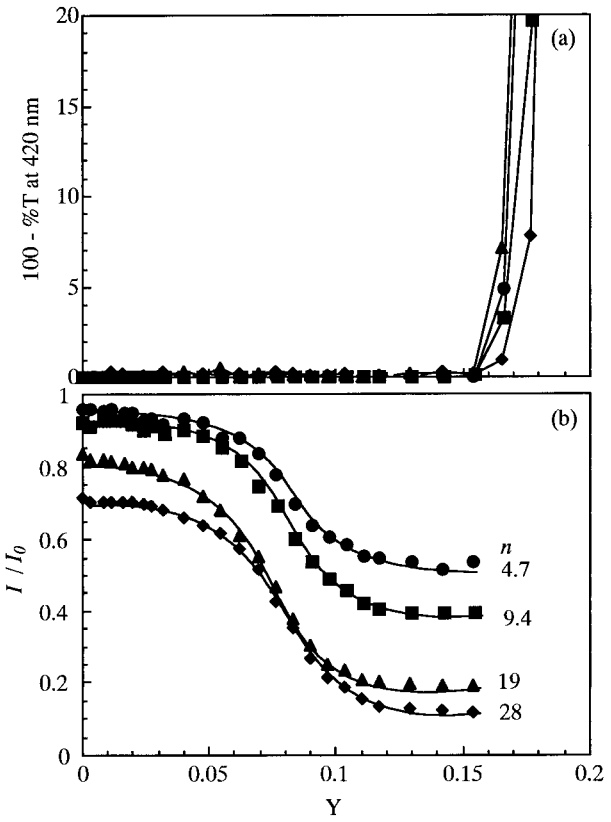

Figure 5. Turbidity (a) and normalized fluorescence intensity (b) as a function of Y for PyPAMPS in the presence of 30 mM DMA-carrying $C_{12}E_6$/CTAC mixed micelle at varying n: [PyPAMPS] = 0.05 g/L and [NaCl] = 0.2 M.

corresponding to an increase in the mean micelle surface charge density. In Figure 5b, the fluorescence intensity, normalized with respect to the value at $Y = 0$ and in the absence of DMA, displays a well-defined break at $Y_c \cong 0.05$, independent of n, and corresponding to the onset of polymer−micelle interaction.[29] At $n > 19$, however, significant quenching is observed at $Y < Y_c$, and the break is less well-defined. This effect probably arises from quenching by DMA in the bulk aqueous phase. In Figure 5a, which shows the effect of Y on turbidity, we observe bulk phase separation of the complex at $Y_p = 0.16 \pm 0.01$. In contrast to other polyion−micelle systems,[8,9,12] Y_c cannot be detected by simple turbidity. In fact, little enhancement of scattering is seen even when the fluorescence results show that nearly all pyrene groups are quenched by micelle binding. This finding suggests that the scattering intensity of the soluble complex formed at $Y_c < Y < Y_p$ is small, either because the molecular mass is low, or because the residence time of bound micelles is short. Results reported elsewhere indicated that micelles bind preferentially to pyrene sites in the region $Y_c < Y < Y_p$, and since the number of pyrene sites per chain is very small, the resulting complexes are not strong scatterers.[29] Along the same line, the relatively large value of Y_p may reveal that subsequent binding of micelles to non-pyrene (AMPS) sites is a precondition for phase separation.[29]

In Figure 6 are plotted the normalized fluorescence intensities against Y at $n = 9.4$ at varying micelle concentrations. It appears that the region of Y in which strong quenching occurs shifts toward lower Y with an increase in the micelle concentration and that the quenching is more gradual at lower micelle concentrations. Furthermore, the quenching increases sigmoidally with

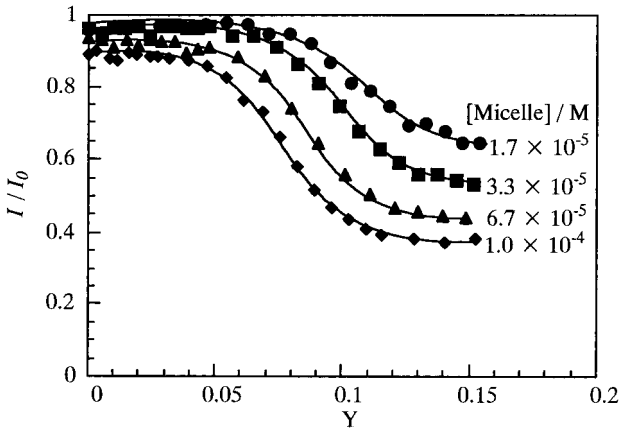

Figure 6. Normalized fluorescence intensity as a function of Y for PyPAMPS in the presence of varying concentrations of DMA-carrying $C_{12}E_6$/CTAC mixed micelle: [PyPAMPS] = 0.05 g/L, $n = 9.4$, and [NaCl] = 0.2 M.

Y and eventually saturates, saturation occurring more readily at higher micelle concentrations. This saturation is observed in Figure 6 only at [micelle] = 1.0×10^{-4} M. As will be explained below, these observations may be rationalized if we consider the data in Figure 6 to represent binding curves and if we take into account the compositional distribution of the micelle as was recently demonstrated by capillary electrophoresis.[30]

We previously observed—in the system comprised of poly(dimethyldiallylammonium chloride) and sodium dodecyl sulfate (SDS)/Triton X-100 mixed micelles—that Y_c, determined turbidimetrically, was independent of micelle concentration.[23,31] This is in contrast to the result shown in Figure 6, in which the onset of binding decreases from Y = ca. 0.06 to 0.035 with increase in micelle concentration. This observation suggests a qualitative difference between Y_c observed by quenching for PyPAMPS and Y_c observed turbidimetrically for a polyelectrolyte with no fluorophore pendant group. We tentatively suggest that the latter is dominated by the cooperative binding of some number of polyion residues and resembles a microscopic phase transition, so that the number of micelles in the system is unimportant. The former situation, on the other hand, is strongly influenced by the interaction of a micelle with a single residue (pyrene-bearing) and therefore exhibits some of the characteristics of a conventional binding equilibrium. In this case, the number of pyrene groups that are micelle-bound depends on both the number concentration of micelles and their binding constant.

The micelle−PyPAMPS binding constant is strongly dependent on Y and is in fact negligibly small for $Y < 0.05$. It is expected to increase with Y for $Y > 0.05$. According to the data in Figure 6, the decrease in binding affinity as Y decreases from ca. 0.12 to ca. 0.10 may be compensated for by an increase in micelle concentration from 3.3×10^{-5} to 6.7×10^{-5} M (these two sets of conditions yield about the same quenching).

At $Y = 0.12$, a micelle concentration of 1.0×10^{-4} M is large enough so that all pyrene groups are micelle-bound. When the concentration of micelles is less than ca. 4×10^{-5} M, Y would have to be increased above ca. 0.20 to achieve this saturation. However, at these larger values of Y, bulk phase separation occurs.

The foregoing explanation accounts for the results by suggesting that the binding affinity changes progressively with Y. However, it is also likely that any given value of

(29) Yoshida, K.; Morishima, Y.; Dubin, P. L.; Mizusaki, M. *Macromolecules* **1997**, *30*, 6208.

(30) Zhang, H.; Dubin, P. L. *J. Colloid Interface Sci.* **1997**, *186*, 264.
(31) Dubin, P. L.; Oteri, R. *J. Colloid Interface Sci.* **1983**, *95*, 453.

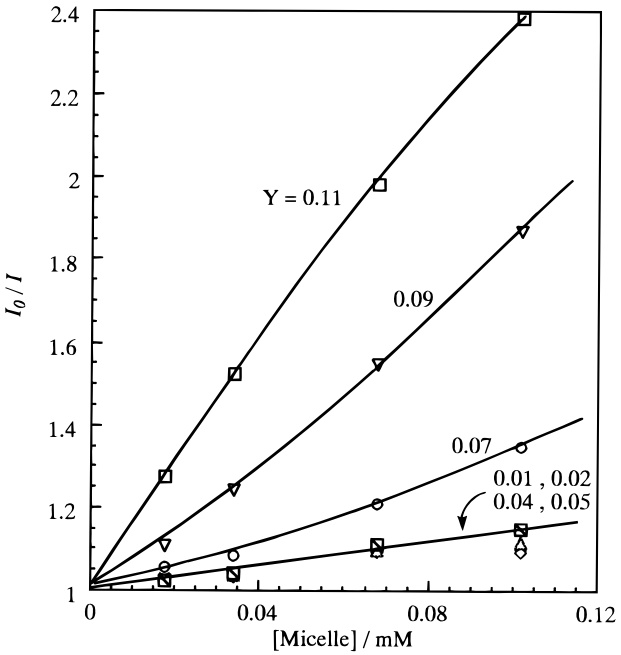

Figure 7. Stern−Volmer plots for fluorescence quenching of PyPAMPS by DMA-carrying $C_{12}E_6$/CTAC mixed micelle at varying *Y*: [PyPAMPS] = 0.05 g/L, n = 9.4, and [NaCl] = 0.2 M.

Y simply represents a stoichiometric average for a system containing a highly polydisperse mixtures of micelles with varying microscopic compositions (y).[30] If we assume that only micelles with a CTAC mole fraction higher than y^* can bind, then the number of micelles with $y > y^*$ increases with increasing *Y* and increasing micelle concentration. Such compositional heterogeneity could yield the observed sigmoidal curves even if binding affinities changed very abruptly with *Y* and the present data do not permit resolution of these two alternatives.

From the data in Figure 6 we obtain a set of Stern−Volmer plots at different *Y* values (Figure 7). The Stern−Volmer plots are nearly collinear at $Y < 0.05$, but the slope increases with *Y* and curvature appears for $Y > 0.05$. These findings indicate that the quenching mechanisms are different at *Y* below and above ca. 0.05 (Y_c). The linear relationship at low *Y*, taken together with the results in Figure 3, implies that fluorescence quenching at $Y < Y_c$ is essentially dynamic and arises from transient collisions between PyPAMPS and DMA-carrying mixed micelles. At larger *Y* (>0.05), the quenching may be due to dynamic association between PyPAMPS and the mixed micelle and the slope may reflect *Y*-dependent binding constants.

When *Y* is further increased to 0.11, the Stern−Volmer plot may exhibit downward curvature. In the present stage of our work, we are unable to discuss quenching mechanisms at $Y > Y_c$. It is, however, possible that fluorescence quenching occurs via two different mechanisms in different two *Y* regions, in addition to the simple collisional quenching at $Y < 0.05$.

Fluorescence Decay. Fluorescence decay measurements may provide useful information about the dynamic state of the polymer−micelle complex. If the residence time of bound DMA-containing mixed micelle is much longer than the fluorescence lifetime of pyrene, then quenching may appear "static" in time-dependent fluorescence. On the other hand, if the residence time is much shorter than the fluorescence lifetime, as is the case of the correlation time for simple collisional encounters, fluorescence quenching should appear "dynamic". In the former case, the peak counts in single-photon counting fluorescence decay measurements may decrease (depending on the time resolution of instruments employed) as quenching increases while the average lifetimes remain more or less the same. In the latter case, however, we will see single-exponential decays with only decreased lifetimes, the peak counts remaining unchanged (if instrumental conditions, including light intensity of a lamp, are kept constant during a whole series of quenching experiments). In the third case, where the residence time of bound micelles is comparable with the fluorescence lifetime of pyrene, the average lifetimes will shorten considerably with increasing extent of quenching, while the peak counts may or may not change depending on the rate of quenching within complexes relative to the time resolution of instruments employed.

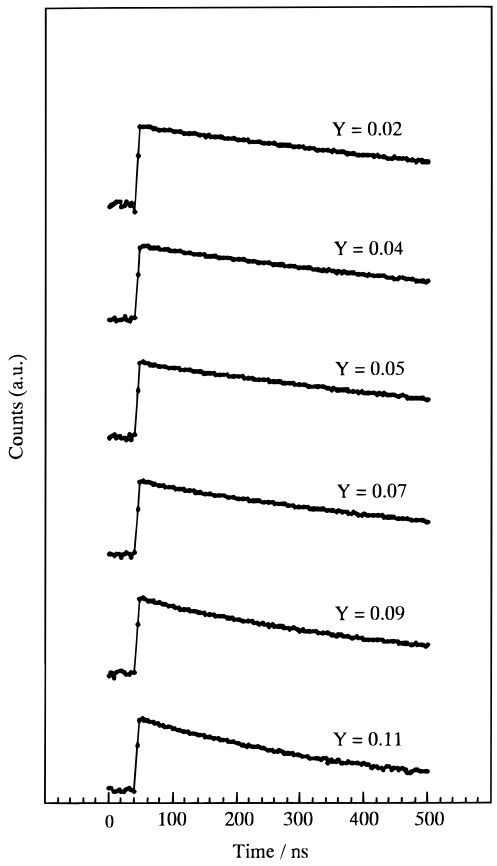

Figure 8. Fluorescence decay profiles for PyPAMPS in the presence of DMA-carrying $C_{12}E_6$/CTAC mixed micelle at varying *Y*: [PyPAMPS] = 0.05 g/L, n = 9, and [NaCl] = 0.2 M.

In Figure 8, fluorescence decay curves for $0.02 < Y < 0.11$ are compared at $[C_{12}E_6] = 30$ mM and $n = 9.4$. The decay curves are reasonably well-fitted with a single-exponential function at $Y < 0.05$, indicating that dynamic fluorescence quenching occurs via collision. At $Y > 0.07$, however, fluorescence lifetimes are significantly shorter and the decays are best fitted by double-exponential functions. The average lifetimes and the peak counts are plotted as a function of *Y* in Figure 9. It appears that the average lifetime begins to decrease significantly near $Y = 0.05$ whereas the peak counts remain the same at $Y < 0.09$. These observations imply a change in quenching process from collisional to complex formation before and after Y_c. It also suggests that quenching is dynamic in the region $0.05 < Y < 0.09$ arising from transient interaction between PyPAMPS and DMA-carrying $C_{12}E_6$/CTAC micelles. At larger *Y*, however, the peak count is slightly smaller than that at $Y < 0.09$, suggesting contribution of static quenching at $Y > 0.11$.

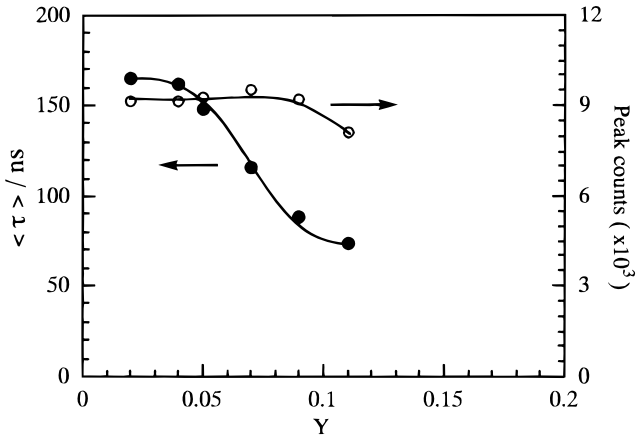

Figure 9. Average lifetime $\langle\tau\rangle$ and peak counts as a function of Y for PyPAMPS in the presence of DMA-carrying $C_{12}E_6$/CTAC mixed micelle: [PyPAMPS] = 0.05 g/L, $n = 9$, and [NaCl] = 0.2 M.

Fluorescence and Absorption Spectra. Fluorescence spectra of the pyrene label provide information about its local environment because the ratio of the third to first vibrational fine structure, I_3/I_1, of the pyrene fluorescence is sensitive to the environmental polarity.[32] It is generally known that the I_3/I_1 ratio is larger in less polar media. The I_3/I_1 ratios of PyPAMPS in the presence of 30 mM quencher-free $C_{12}E_6$/CTAC at varying Y are plotted in Figure 10. At micelle concentrations higher than 6.7×10^{-5} M, the I_3/I_1 ratios are constant at $Y < 0.05$ but decrease in the region $0.05 < Y < 0.11$ and saturate at $Y >$ ca. 0.11. These I_3/I_1 curves strongly resemble the I/I_0 curve at [micelle] $= 1.0 \times 10^{-4}$ M in Figure 6, the Y value at which the I_3/I_1 and I/I_0 values commence to decrease corresponding to Y_c observed by fluorescence quenching. At lower micelle concentrations, the decreases in I_3/I_1 is more gradual. This trend may be explained in terms of a compositional distribution of micelles as discussed above.

The decrease in the I_3/I_1 ratio with increasing Y was the opposite tendency that we had anticipated because the hexa(oxyethylene) phase was thought to be less polar than water. In a separate experiment, we measured fluorescence and absorption spectra of PyPAMPS in mixtures of water and polyethylene glycol (PEG) (average molecular weight, ca. 500) at varying compositions. As can be seen in Figure 11, as the weight fraction of PEG is increased, I_3/I_1 decreases while the absorption maximum for the pyrene 0−0 band increases. The magnitude of the drop in I_3/I_1 in excess PEG is essentially equal to that observed in Figure 10 upon increase in Y. These observations indicate that pyrene labels are incorporated in the hexa(oxyethylene) layer in $C_{12}E_6$/CTAC mixed micelles when complexes are formed at $Y > 0.05$.

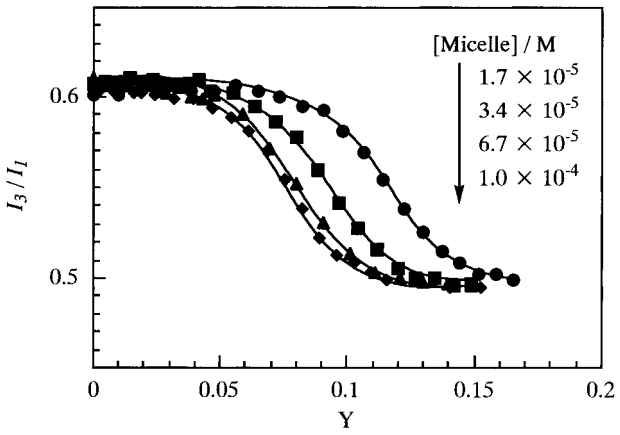

Figure 10. I_3/I_1 ratio as a function of Y for PyPAMPS in the presence of varying concentrations of $C_{12}E_6$/CTAC mixed micelle: [PyPAMPS] = 0.05 g/L and [NaCl] = 0.2 M.

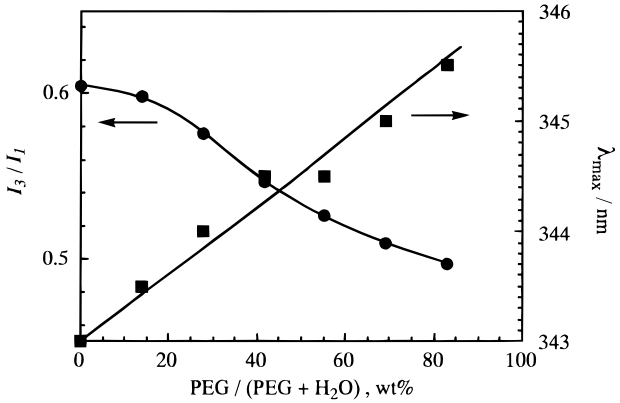

Figure 11. I_3/I_1 ratio and λ_{max} for PyPAMPS as a function of the weight percent of PEG in the PEG/water mixture.

Acknowledgment. This work was supported in part by a Grant-in-Aid for Scientific Research on Priority Areas, "New Polymers and Their Nano-Organized Systems" (No. 277/08246236), from The Ministry of Education, Science, Sports, and Culture, Japan.

LA970780Y

(32) Kalyanasundaram, K.; Thomas, J. K. *J. Am. Chem. Soc.* **1977**, *99*, 2039.